CFD Letters 13, Issue 10 (2021) 52-68

CFD Letters

Journal homepage:
https://semarakilmu.com.my/journals/index.php/CFD_Letters/index
ISSN: 2180-1363

Effect of Expansion Direction/Area Ratio on Loss Characteristics and Flow Rectification of Curve Diffuser

Teo Wen Yong[1], Normayati Nordin[1,*], Bukhari Manshoor[1], Zainal Ambri Abdul Karim[2], Shamsuri Mohamed Rasidi[1], Hau Chin Yong[1], Muhammad Zahid Firdaus Shariff[1], Muhammad Musleh Anuar[1]

[1] Centre for Energy and Industrial Environment Studies, Faculty of Mechanical and Manufacturing Engineering, Universiti Tun Hussein Onn Malaysia, 86400 Batu Pahat, Johor Darul Takzim, Malaysia
[2] Department of Mechanical Engineering, Faculty of Engineering, Universiti Teknologi PETRONAS, 32610 Seri Iskandar, Perak Darul Ridzuan, Malaysia

ARTICLE INFO

Article history:
Received 16 July 2021
Received in revised form 3 September 2021
Accepted 17 September 2021
Available online 31 October 2021

Keywords:
Curve Diffuser; Area Ratio; Pressure Recovery; Flow Uniformity

ABSTRACT

Curve diffuser is frequently used in applications such as HVAC, wind- tunnel, gas turbine cycle, aircraft engine etc. as an adapter to join the conduits of different cross-sectional areas or an ejector to decelerate the flow and raise the static pressure before discharging to the atmosphere. The performance of the curve diffuser is greatly affected by the abrupt expansion and inflection introduced, particularly when a sharp 90^{o} curve diffuser is configured with a high area ratio (AR). Therefore, the paper aims to numerically investigate the effect of the expansion direction of AR=1.2 to 4.0 curve diffuser on loss characteristic and flow rectification. 90^{o} curve diffuser operated at inflow Reynolds Number, Re_{in}=5.934 × 10^{4} to 1.783 × 10^{5} was considered. Results show that pressure recovery improves when the area ratio increases from 1.2 to 2.16 for both 2D expansion (z- direction) and 3D expansion (x- and z- direction). On the other hand, the increase of inflow Reynolds number causes the flow uniformity to drop regardless of the expansion directions. 3D expansion (x- and z- direction) curve diffuser with AR=2.16, operated at Re_{in}=8.163 × 10^{4}, is opted as the most optimum, producing the best pressure recovery up to 0.380. Meanwhile, 2D expansion (z-direction) curve diffuser of AR=2.16, , operated at Re_{in}= 5.934 × 10^{4}, is chosen to provide the best flow uniformity of 2.330 m/s. 2D expansion (x- direction) should be as best avoided as it provides the worst overall performance of 90^{o} curve diffuser.

1. Introduction

A diffuser is a device commonly used to reduce velocity and increase the static pressure of a fluid passing through a system by increasing the cross-sectional area. There are various types of the diffuser, classified by its geometry, among others straight diffuser, curve diffuser, annular diffuser, pyramidal diffuser, S-shape diffuser etc. These diffusers are applied in different applications such as HVAC, wind-tunnel, aircraft engine and gas turbine, wherein satisfying its performances to achieve a compromise between pressure recovery and flow uniformity always becomes the main aim [1–6].

* *Corresponding author.*
E-mail address: mayati@uthm.edu.my (Normayati Nordin)

https://doi.org/10.37934/cfdl.13.10.5268

The basic mechanism is by setting geometrical and operating parameters such as area ratio (AR), curvature length (L_{in}/W_1), angle of turn ($\Delta\phi$), turbulent intensity (I) and inflow Reynolds number (Re_{in}) optimally. Failure of doing so may considerably affect the overall performance particularly when a sharp 90^o curve diffuser with a high area ratio is involved [7]. Due to the sharp curvature turn, the inner wall boundary layer thickens, the potential flow loading increases and the turbulent mixing along the inner wall reduces. As a consequence, the fast stream flow deflects much toward the outer wall to produce excessive flow separation and unfavourable flow uniformity.

In some circumstances there would be no relaxation in terms of geometrical selection in spite of a debatable performance owing to design and space constraints. For instance, on account of a space limitation, a 90^o curve diffuser with an extremely short inner wall length (L_{in}/W_1 = 2.6) and large area ratio (AR = 3.9) was designed, though unfavourable for a blow-down wind tunnel system [8]. Despite a deficient performance, an 180^o curve diffuser with inner wall expansion and large AR = 4.0 was still introduced for a wind tunnel application due to a design restriction [9].

There are abundant works done previously to investigate the effects of geometrical and operating parameters on diffuser performances [10–20], but none has focused on the effects of area ratio (AR) configured with different expansion directions, i.e. 2D expansion (z- direction), 3D expansion (x- and z- direction), 2D expansion (x- direction) and inflow Reynolds Number (Re_{in}). Therefore, this study aims to numerically investigate the effects of expansion directions of 90^o curve diffuser with AR= 1.2, 1.6, 2.16, 3.0, 4.0 and Re_{in}= 5.934 × 10^4, 8.163 × 10^4, 1.783 × 10^5 on pressure recovery and flow uniformity. These ranges of variables are opted to serve common operating settings of curve diffuser for subsonic applications such as wind tunnel and HVAC systems [7-20].

2. Methodology

ANSYS CFD code FLUENT was used as a tool to simulate the effects of expansion direction/area ratio on curve diffuser performances. Figure 1 illustrates the overall CFD workflow that involves pre-processing, processing and post-processing phases. A sharp 90^o curve diffuser shown in Figure 2 was considered to configure with AR of 1.2, 1.6, 2.16, 3.0 and 4.0 with different expansion directions, 2D expansion (z- direction), 3D expansion (x- and z- direction), 2D expansion (x- direction).

2.1 Modelling and Meshing

Table 1 shows that each area ratio was modelled to configure with all types of expansion. Hybrid mesh to consist of hexahedral and tetrahedral elements was generated to provide acceptable quality of skewness less than 0.3. Near-wall treatments, standard wall function (y+= 64) and enhanced wall treatment (y+= 1.1 to 1.6) were considered to opt the best could resemble the actual case (see Figure 3). Grid independence test was conducted as depicted in Table 2 with Mesh 4 was opted to provide the least deviation relative to the finest mesh within reasonable CPU solving time.

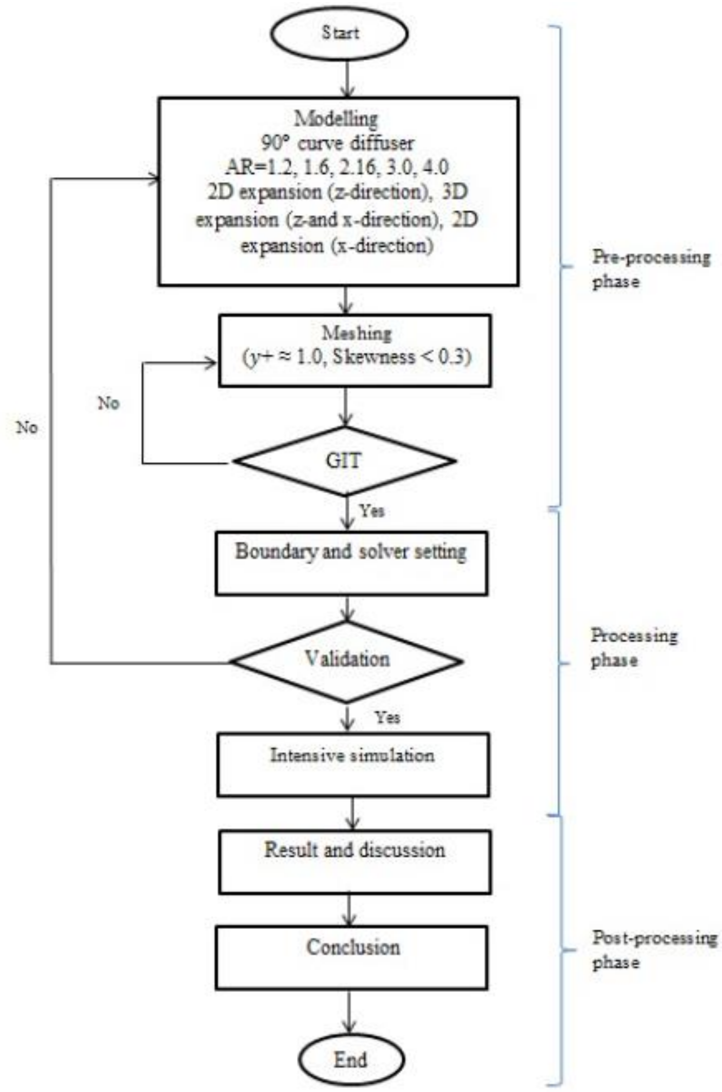

Fig. 1. Methodology flow chart

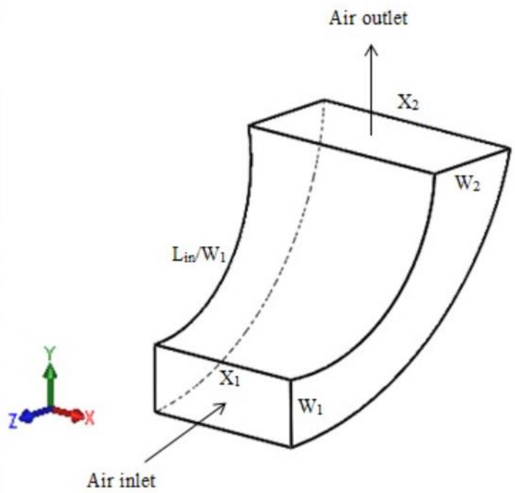

2D expansion (x- direction)	Expansion along x-axis (inner wall expansion)
2D expansion (z- direction)	Expansion along z-axis (side expansion)
3D expansion (x- and z- direction)	Expansion along both x- and z-axis

Fig. 2. 90° curve diffuser

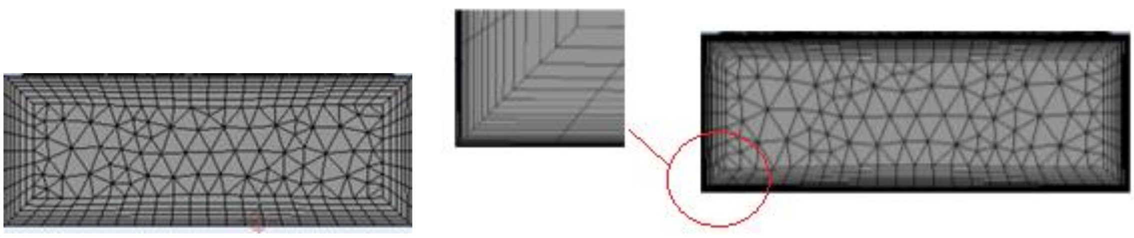

(a) (b)

Fig. 3. Near wall treatments (a) standard wall function($y+= 64$) and (b) enhanced wall treatment ($y+= 1.1$ to 1.6)

Table 1
Curve diffuser models

AR	2D expansion (z- direction)	3D expansion (both z- and x- direction)	2D expansion (x- direction)
1.2	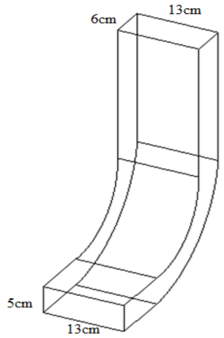	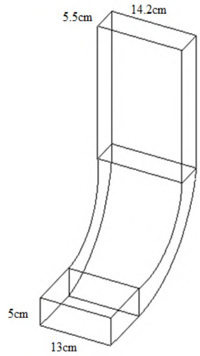	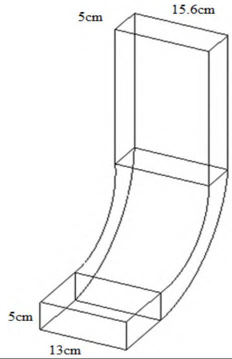
2.16	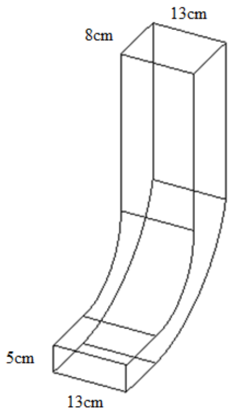	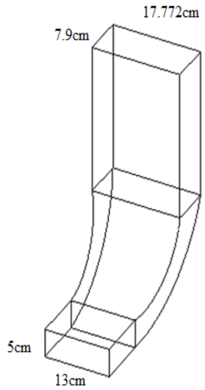	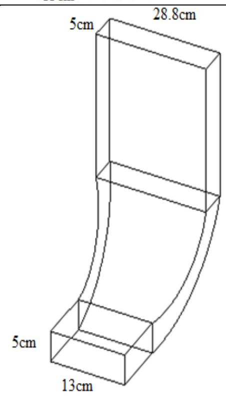
4.0	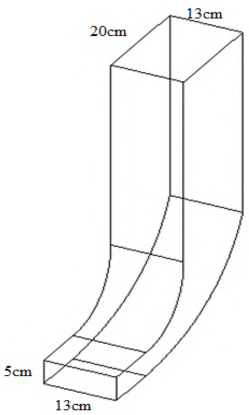	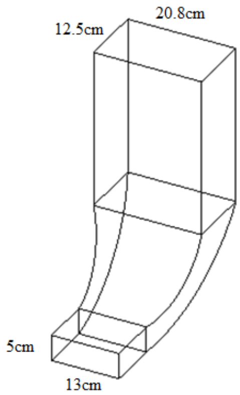	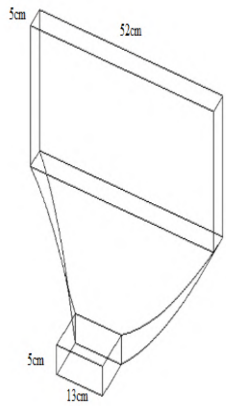

Table 2
Grid independency test

Near wall treatment	Mesh	Elements	Nodes	C_p	Dev (%)
Standard wall function	1	402454	151032	0.561	0.43
	2	421337	157560	0.561	0.28
	3	446139	166700	0.561	0.27
	4	468053	174140	0.562	0.09
	5	504774	188227	0.563	-
Enhanced wall treatment	1	513574	245024	0.165	42.76
	2	599759	265591	0.202	29.58
	3	736100	350067	0.242	15.76
	4	908103	431169	0.275	4.25
	5	1157422	548239	0.287	-

2.2 Solver and Boundary Condition Settings

The following three-dimensional steady-state Reynolds Averaged Navier Stokes (RANS) equations were numerically solved for a Newtonian, incompressible fluid. The flow was assumed to be fully developed, steady-state and isothermal. The gravitational effect was negligible.

Continuity equation

$$\frac{\partial u}{\partial x}+\frac{\partial v}{\partial y}+\frac{\partial w}{\partial z}=0 \quad (1)$$

X-momentum equation

$$u\frac{\partial u}{\partial x}+v\frac{\partial u}{\partial y}+w\frac{\partial u}{\partial z}=-\frac{1}{p}\frac{\partial p}{\partial x}+v\left[\frac{\partial^2 u}{\partial x^2}+\frac{\partial^2 u}{\partial y^2}+\frac{\partial^2 u}{\partial z^2}\right]+\frac{1}{p}\left[\frac{\partial(-p\overline{u'^2})}{\partial x}+\frac{\partial(-p\overline{u'v'})}{\partial y}+\frac{\partial(-p\overline{u'w'})}{\partial z}\right] \quad (2)$$

Y-momentum equation

$$u\frac{\partial v}{\partial x}+v\frac{\partial v}{\partial y}+w\frac{\partial v}{\partial z}=-\frac{1}{p}\frac{\partial p}{\partial y}+v\left[\frac{\partial^2 v}{\partial x^2}+\frac{\partial^2 v}{\partial y^2}+\frac{\partial^2 v}{\partial z^2}\right]+\frac{1}{p}\left[\frac{\partial(-p\overline{u'v'})}{\partial x}+\frac{\partial(-p\overline{v'^2})}{\partial y}+\frac{\partial(-p\overline{v'w'})}{\partial z}\right] \quad (3)$$

Z-momentum equation

$$u\frac{\partial w}{\partial x}+v\frac{\partial w}{\partial y}+w\frac{\partial w}{\partial z}=-\frac{1}{p}\frac{\partial p}{\partial z}+v\left[\frac{\partial^2 w}{\partial x^2}+\frac{\partial^2 w}{\partial y^2}+\frac{\partial^2 w}{\partial z^2}\right]+\frac{1}{p}\left[\frac{\partial(-p\overline{u'w'})}{\partial x}+\frac{\partial(-p\overline{v'w'})}{\partial y}+\frac{\partial(-p\overline{w'^2})}{\partial z}\right] \quad (4)$$

As listed in Table 3, three types of boundary operating conditions were imposed. The inlet velocity, V_{in} was varied in the range 13.26 to 39.83 m/s corresponding to the Re_{in} = 5.934x10^4 – 1.783x10^5 and I_{in} = 3.7 - 4.1. At the outlet boundary, the pressure was set at atmospheric pressure (0 gage pressure). At the solid wall, the velocity was zero due to the no-slip condition.

Table 3
Boundary conditions

Inlet	Type of boundary	Velocity inlet
	Velocity magnitude, V_{in} (m/s)	13.26m/s (5.934x10^4)
		18.23m/s (8.162x10^4)
		39.83m/s (1.783x10^5)
	Turbulent intensity, I_{in} (%)	4.1
		3.9
		3.7
	Hydraulic diameter, D_h (mm)	72
Outlet	Type of boundary	Pressure outlet
	Pressure (Pa)	Zero-gauge pressure
Wall	Type of boundary	Smooth wall
	Shear condition	No-slip condition
Working Fluid Properties	Working fluid	Air
	Temperature (°C)	30
	Density, ρ (kg/m^3)	1.164
	Dynamic viscosity, μ (kg/m. s)	1.872x10^{-5}

Table 4 lists the details of the solver setting applied. The governing equations were independently solved using a double-precision pressure-based solver with a robust pressure-velocity coupling algorithm, SIMPLE been applied. To reduce numerical diffusion, the QUICK scheme was employed for the discretization of the momentum equations, the turbulent kinetic energy equation, and the turbulent dissipation rate equation. A PRESTO discretization scheme was applied for the continuity equation and a default scheme, i.e. Green-Gauss Cell-based, was employed for the solution of the gradient. Standard k-ε (ske) turbulence model equipped with near-wall treatments, standard and enhanced were considered for the validation. The most optimum solution setting shall provide the least discrepancies with similarity of flow characteristics to the experiment.

Table 4
Solver details

Solver Scheme	SIMPLE
Gradient	Green-Gauss Cell Based
Pressure	PRESTO
Momentum	QUICK
Turbulent Kinetic Energy	QUICK
Turbulent Dissipation Rate	QUICK
Turbulence models	Standard k-ε (ske) model
Near wall treatment	Standard wall function Enhanced wall treatment (EWT)

Pressure recovery coefficient (C_p) and flow uniformity index (σ_{out}) are defined as follows

$$Cp = \frac{2(P_{out} - P_{in})}{\rho {V_{in}}^2} \quad (5)$$

where, P_{out} = Average static pressure at outlet (Pa); P_{in} = Average static pressure at inlet (Pa); ρ = Air density (kg/m^3); V_{in} = Mean air velocity at inlet (m/s)

$$\sigma_{out} = \sqrt{\frac{1}{N-1}\sum_{i=1}^{N}(V_i - V_{out})^2} \quad (6)$$

where, N = Number of measurement points; V_i = Local air velocity at outlet (m/s); V_{out} = Mean air velocity at outlet (m/s)

The C_p indicates how much kinetic energy is successfully converted to pressure energy. The main problem in achieving high pressure recovery is flow separation, which results in dissipation of energy and non-uniform flow distribution [21-23]. The σ_{out} is used to measure the dispersion of local velocity from the mean velocity. It is strongly dependent on the distribution of the core flow and the presence of secondary flow. The flow is considered uniform with the presence of secondary flow of less than 10% [24-26].

2.3 Numerical Validation

For validation, ske turbulence model adopted both standard and enhanced wall treatment was considered. Previous experimental work by Rasidi *et al.,* [15] was referred to validate the best model to represent the case. As shown in Figure 4, ske turbulence model equipped with enhanced wall treatment resembles well the experimental case with a deviation percentage of approximately 0.83%.

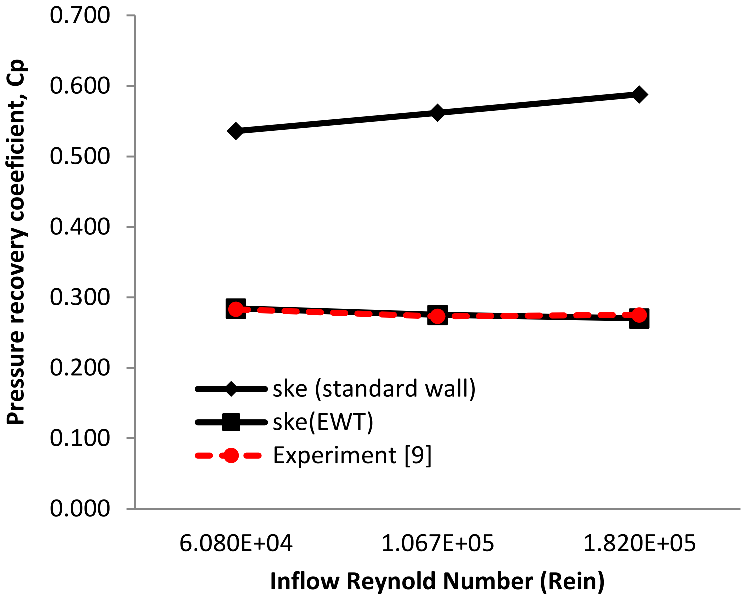

Fig. 4. Numerical validation

3. Results and Discussion

Effects of area ratio configured with different expansion direction and inflow Reynold number on pressure recovery and flow uniformity are assessed. Ultimately, the most optimum configuration is proposed.

3.1 Effect of Area Ratio on Pressure Recovery of Different Expansion Curve Diffuser

Figure 5 shows the effects of area ratio on pressure recovery of 2D expansion (z- direction), 3D expansion (x- and z- direction) and 2D expansion (x- direction) curve diffuser at different Re_{in}. Pressure recovery improves with the increase of AR from 1.2 to 2.16 regardless of the expansion types, with the 3D expansion provides the highest recovery of 0.384. Further increase AR to 4.0 considerably reduces the C_p with the 2D expansion (x-direction) is the worst affected. Applying higher Re_{in} is seen to degrade more the performance.

Fundamentally, pressure is recovered when the cross-sectional area increases. However, the vast expansion is always associated with the existence of flow separation, wherein could deteriorate the recovery. As shown in Table 5, AR= 4.0 relatively forms substantial flow separation within the inner wall region. This undesirable flow phenomenon is not only to disrupt the pressure recovery but more importantly to damage the downstream equipment and generate structural vibration.

Despite the 2D expansion (x- direction) is found to experience the worst pressure recovery, the velocity vector at centre longitudinal plane shown in Table 5 demonstrates otherwise, with minimal flow separation is occurred. To justify this, further assessment is performed by examining the flow physics of different views (see Figure 6). It is observed that, due to the inner wall expansion, 2D expansion (x-direction) experiences flow complexity with the presence of flow separation and secondary flow vortices at both left and right sides of expansion.

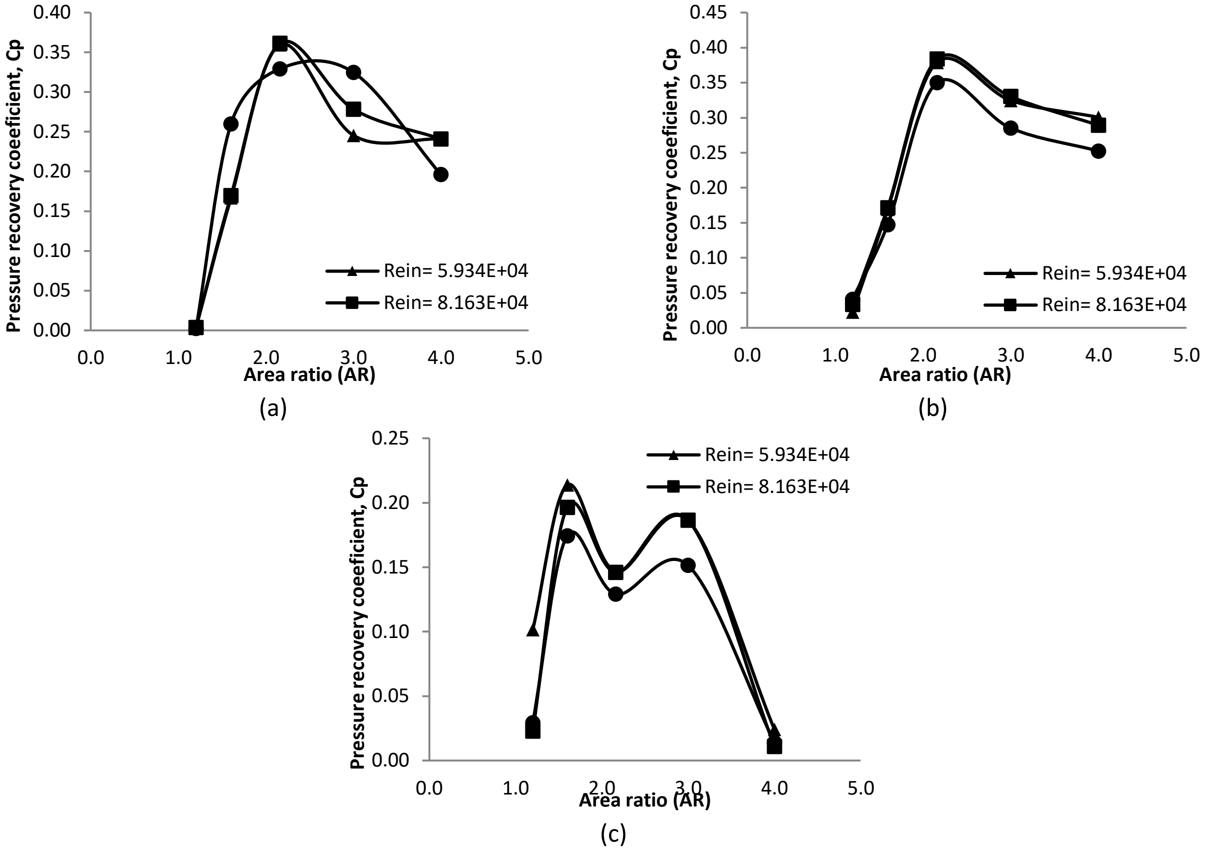

Fig. 5. Effects of area ratio on pressure recovery of (a) 2D expansion (z-direction) (b) 3D expansion (x- and z-direction) and (c) 2D expansion (x-direction) at different inflow Reynolds Number

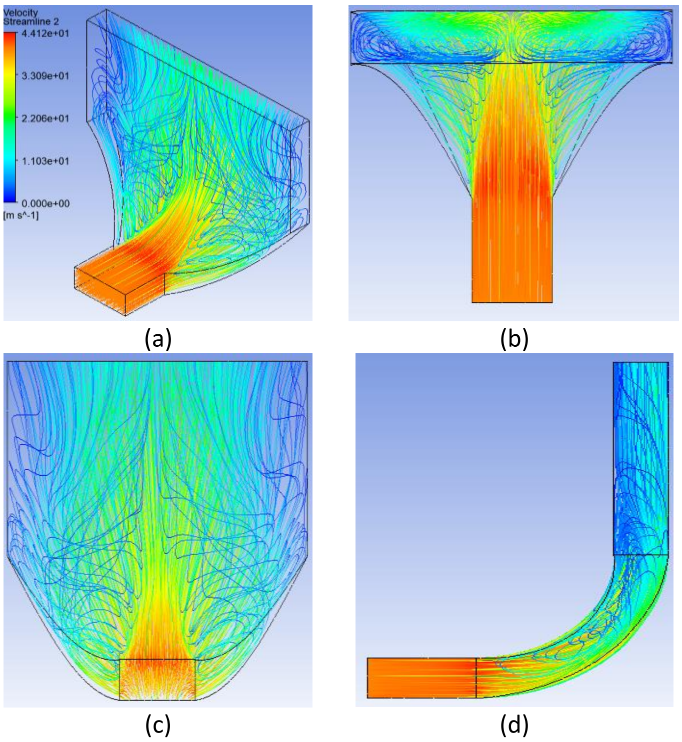

Fig. 6. 90° curve diffuser with the worst pressure recovery (AR=4.0, 2D expansion x- direction, Re_{in}=8.364 x10^4) (a) isometric (b) plan (c) frontal and (d) side views

Table 5
Velocity vector of 90° curve diffuser with AR= 1.2, 2.16, 4.0 operated at Re_{in}=5.934 x 10^5

<table>
<tr><th>AR</th><th>2D expansion (z- direction)</th><th>3-D expansion (x- and z- direction)</th><th>2D expansion (x-direction)</th></tr>
<tr><td>1.2</td><td>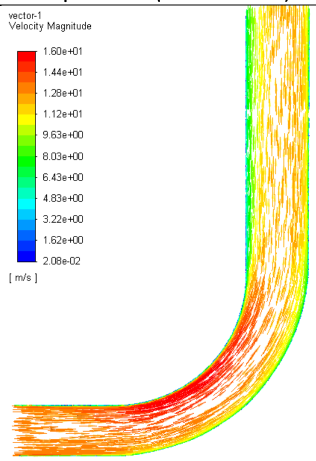
</td><td>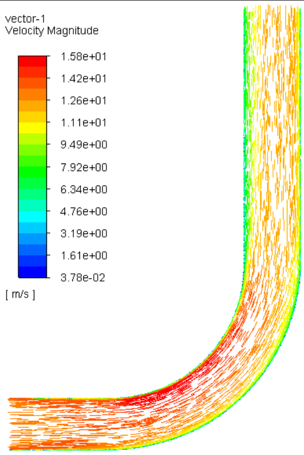
</td><td>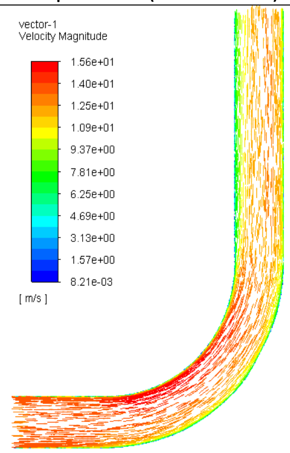
</td></tr>
<tr><td>2.16</td><td>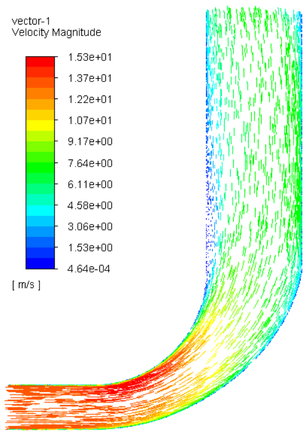
</td><td>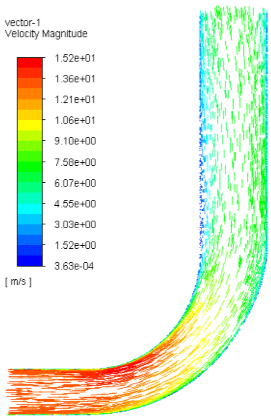
</td><td>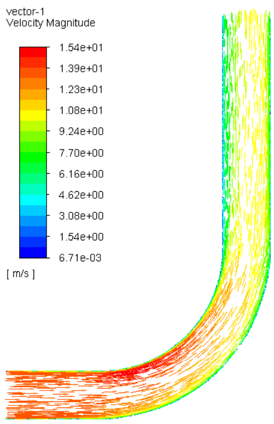
</td></tr>
<tr><td>4.0</td><td>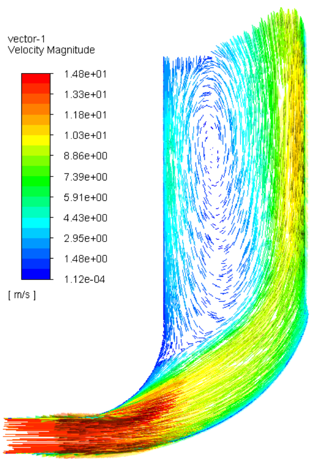
</td><td>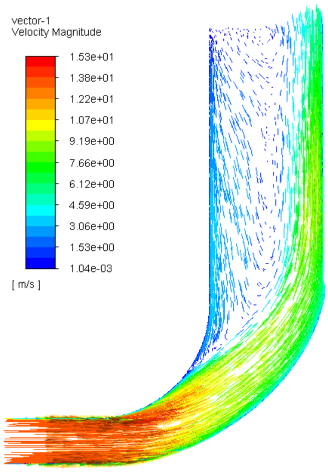
</td><td>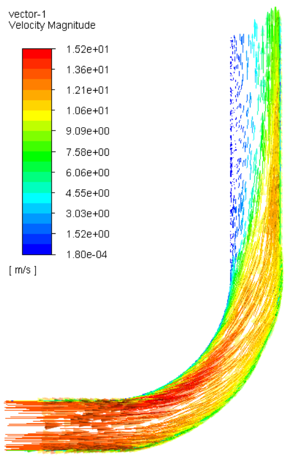
</td></tr>
</table>

3.2 Effect of Area Ratio on Flow Uniformity of Different Expansion Curve Diffuser

Figure 7 shows the effects of area ratio on flow uniformity of 2D expansion (z- direction), 3D expansion (x- and z- direction) and 2D expansion (x- direction) curve diffuser at different Re_{in}. It is seen that the flow uniformity is governed more by Re_{in} than AR. Applying relative high Re_{in} severely distorts the flow uniformity. It is worth noted the higher the σ_{out}, the severer the flow uniformity.

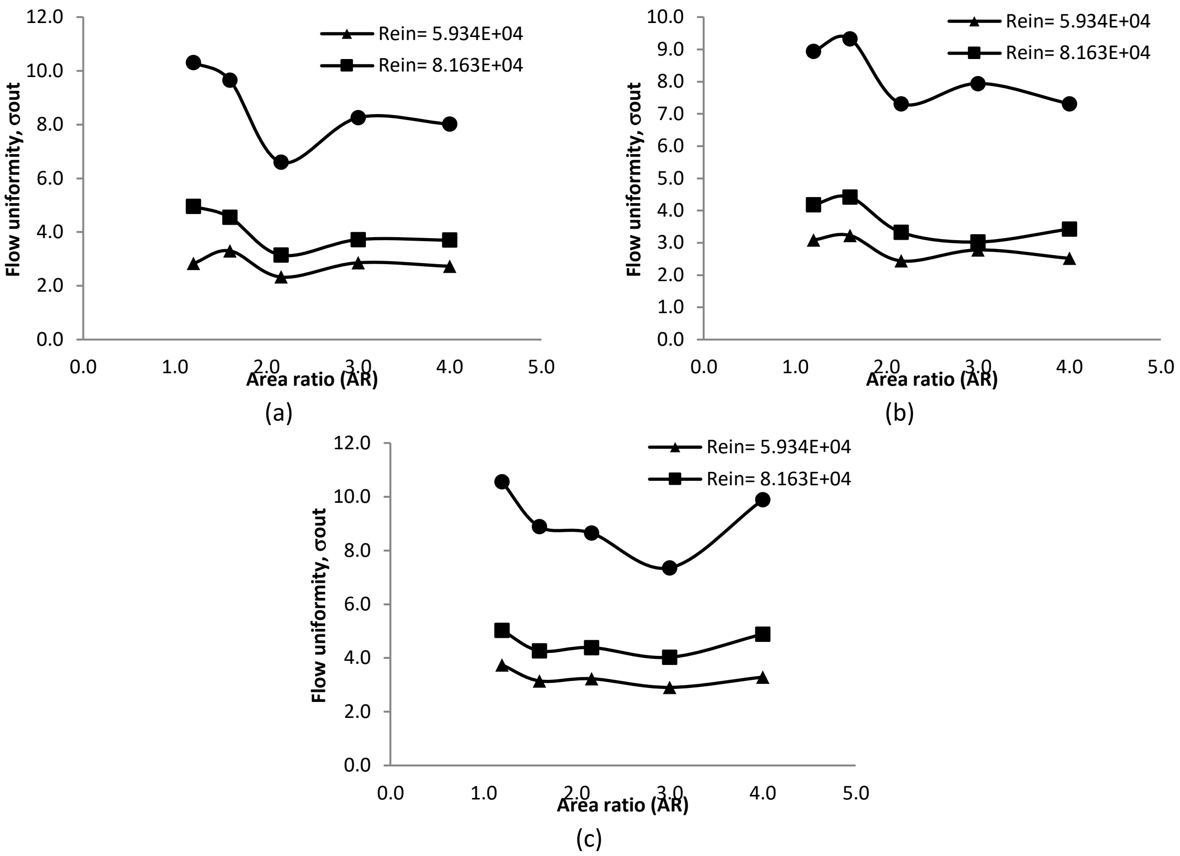

Fig. 7. Effects of area ratio on flow uniformity of (a) 2D expansion (z-direction) (b) 3D expansion (x- and z-direction) and (c) 2D expansion (x-direction) at different inflow Reynolds Number

As shown in Table 6, both AR= 2.16 and 4.0 share almost similar flow characteristics at the outlet, wherein due to turning and expansion effects, the boundary layer thickens hence form a strong adverse pressure gradient region. At a certain point in this region, flow losses its energy to escalate the boundary thus detaches from the wall with the fast stream tends to deflect to the outer wall and flow is reversed at the inner wall to form severe stall and vortices. Flow uniformity of AR= 4.0 is found to be more affected particularly when 2D inner wall expansion, i.e. x- direction is applied. The flow separation and vortices are found to take place dominantly at both inner wall expansion sides shown in Figure 8.

Both 2D expansion (z-direction) and 3-D expansion (x- and z- direction) shows promising flow uniformity in which selection of the appropriate diffuser should be based on the needs and application constraints.

Table 6
Outlet velocity contour of 90° curve diffuser of AR=2.16, 4.0 operated at Rein= 1.783x10^5

AR	2D expansion (z- direction)	3-D expansion (x- and z- direction)	2D expansion (x-direction)
2.16	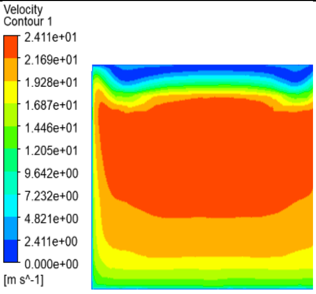	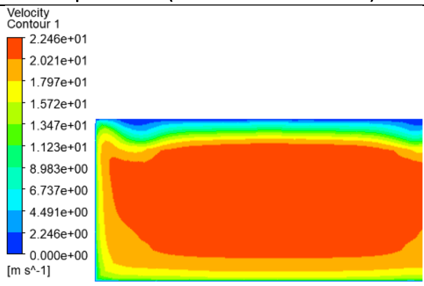	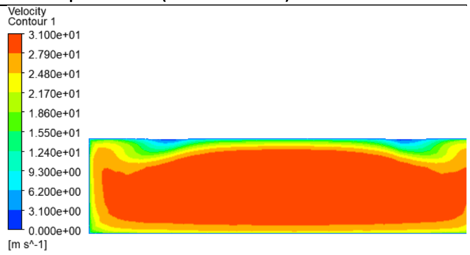
4.0	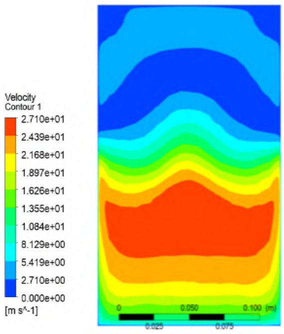	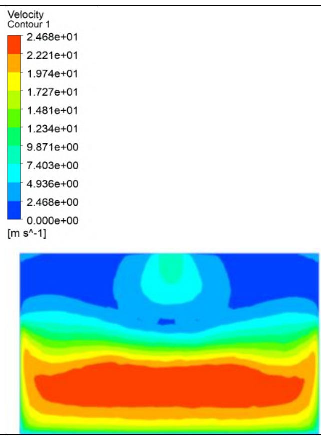	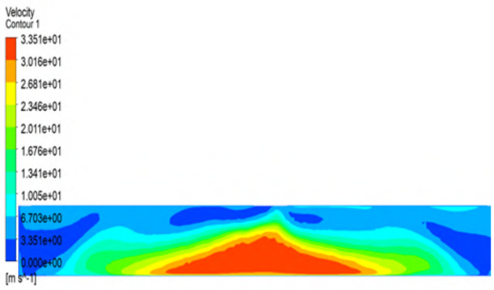

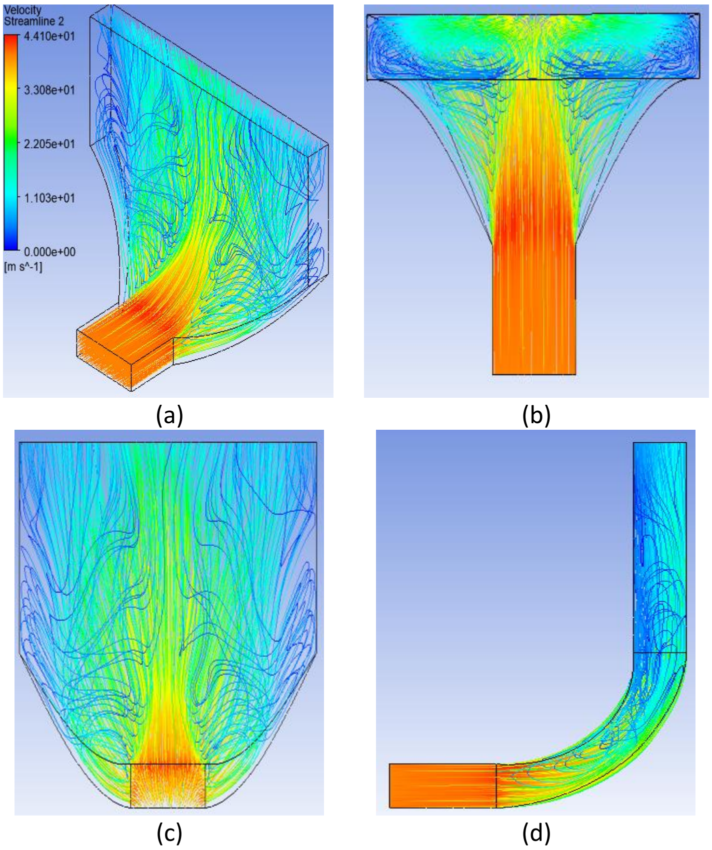

Fig. 8. 90° curve diffuser with the worst flow uniformity (AR=4.0, 2D expansion x- direction Rein=1.783 x10^5) (a) isometric (b) plan (c) frontal and (d) side views

3.3 Effect of Area Ratio on Onset Flow Separation of Different Expansion Curve Diffuser

Table 7 shows the effects of area ratio on onset flow separation (S) of 2D expansion (z- direction), 3D expansion (x- and z- direction) and 2D expansion (x- direction) curve diffuser at different Re_{in}. It is observed that flow separation starts to occur close to the outlet, S= $0.807L_{in}/W_1$ when AR of 2.16 is introduced for 2D expansion (z-direction). This result meets the finding obtained by Fox and Kline [13] to apply AR within 1.2-2.0 for a sharp 90° curve diffuser, otherwise severe stall occurs.

Meanwhile, no separation is found within the central longitudinal section of the inner wall for both 3-D expansion (x- and z-direction) and 2D expansion (x- direction) until respectively at AR 3.0 and 4.0. Table 8 provides the streamline to locate the onset flow separation point. This streamline which was taken at the central longitudinal section of the diffuser, however, is found insufficient to provide comprehensive judgement to the flow physics particularly when a diffuser with inner wall expansion, i.e. x-direction is involved. Hence, three-dimensional flow views should be scrutinized (see Figures 6 and 8). As discussed previously, the diffuser with inner wall expansion is susceptible to extensive flow separation and secondary flow vortices occurred at both sides of expansion, whereby could not be captured by the centre longitudinal two-dimensional plane.

Table 7
Effects of area ratio on onset flow separation of 2D expansion (z-direction), 3D expansion (x- and z-direction) and 2D expansion (x-direction) at different inflow Reynolds Number

AR	Re_{in}	Onset flow separation (S)		
		2D expansion (z- direction)	3D expansion (x- & z- direction)	2D expansion (x- direction)
1.2	5.9343×10^4	-	-	-
	8.1628×10^4	-	-	-
	1.7831×10^5	-	-	-
1.6	5.9343×10^4	-	-	-
	8.1628×10^4	-	-	-
	1.7831×10^5	-	-	-
2.16	5.9343×10^4	$0.807L_{in}/W_1$	-	-
	8.1628×10^4	$0.807L_{in}/W_1$	-	-
	1.7831×10^5	$0.807L_{in}/W_1$	-	-
3.0	5.9343×10^4	$0.645L_{in}/W_1$	$0.718L_{in}/W_1$	-
	8.1628×10^4	$0.645L_{in}/W_1$	$0.703L_{in}/W_1$	-
	1.7831×10^5	$0.645L_{in}/W_1$	$0.678L_{in}/W_1$	-
4.0	5.9343×10^4	$0.407L_{in}/W_1$	$0.618L_{in}/W_1$	-
	8.1628×10^4	$0.407L_{in}/W_1$	$0.593L_{in}/W_1$	-
	1.7831×10^5	$0.407L_{in}/W_1$	$0.528L_{in}/W_1$	$0.923L_{in}/W_1$

Table 8
Streamline of 90° curve diffuser with AR= 1.2, 2.16, 4.0 operated at Re_{in}=1.738 x 10^5

AR	2D expansion (z- direction)	3-D expansion (x- and z- direction)	2D expansion (x-direction)
1.2	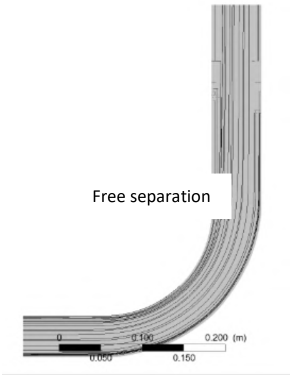	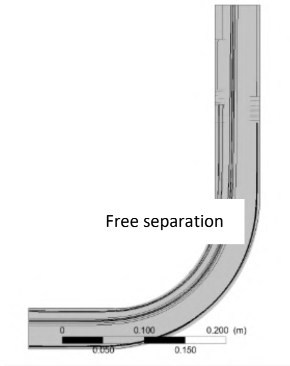	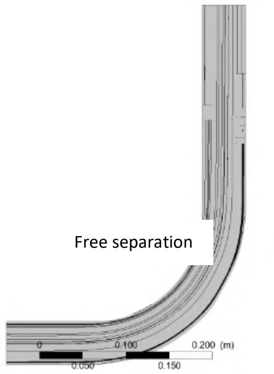
2.16	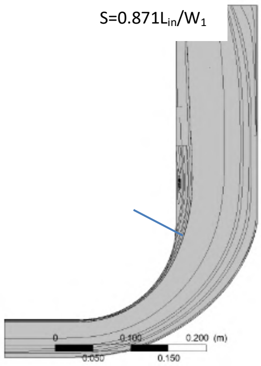	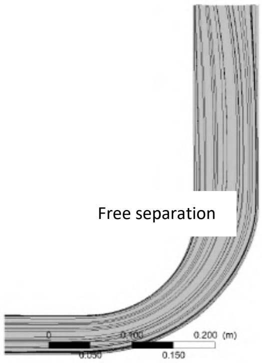	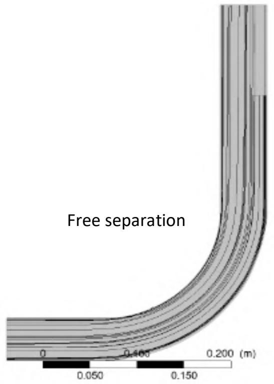
4.0	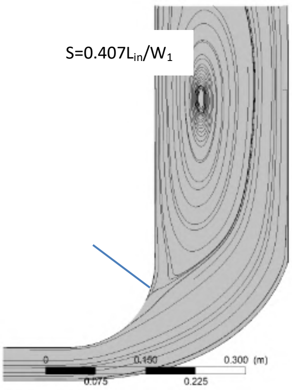	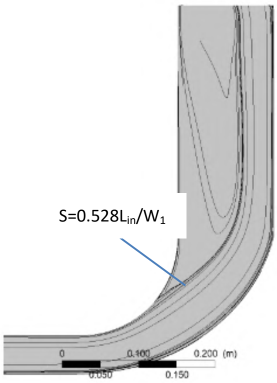	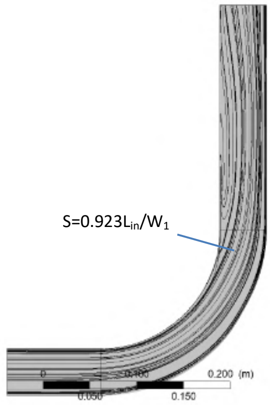

3.4 Optimum Configuration

Table 9 outlines the performance status of 90° curve diffuser with expansion direction (2D z-direction, 3D x- and z- direction, 2D x- direction), area ratio (1.2- 4.0) and inflow Reynolds Number (5.934 x 10^4-1.738 x 10^5).

In terms of pressure recovery, 3D expansion (x- and z- direction) with AR of 2.16 is optimal for producing recovery up to 0.384 operated at Re_{in}=8.163 × 10^4. However, the flow uniformity index obtained is 3.33. In terms of flow uniformity, AR=2.16, 2D expansion z- direction, operated at Re_{in}= 5.9343 × 10^4 is the considered configuration due to promising flow uniformity of 2.33. Eventually, the pressure recovery obtained is 0.360.

There are insignificant differences between these two promising curved diffusers, i.e. 2D expansion (z- direction) and 3D expansion (x- and z- direction) in terms of pressure recovery and flow uniformity. Therefore, a compromise between the maximum permissible pressure recovery and flow uniformity is determined to be based upon the need. Whenever the pressure recovery is of interest it is promising to apply the 3D curved diffuser with Re_{in} = 8.163 × 10^4 and AR= 2.16. If the flow uniformity is the primary concern, it is viable to opt for the 2D expansion z- direction curved diffuser with Re_{in} = 5.9343 ×10^4 and AR= 2.16. Figures 9 and 10 illustrate the flow characteristics of both promising configurations. The streamlines are in order with no/minimal presence of stalls and vortices.

As depicted in Table 10, the 2D expansion (x- direction) is found to produce the worst overall performance for both recovery and uniformity relatively up to 50% and 15%. Therefore, this type of expansion direction should as best not be opted.

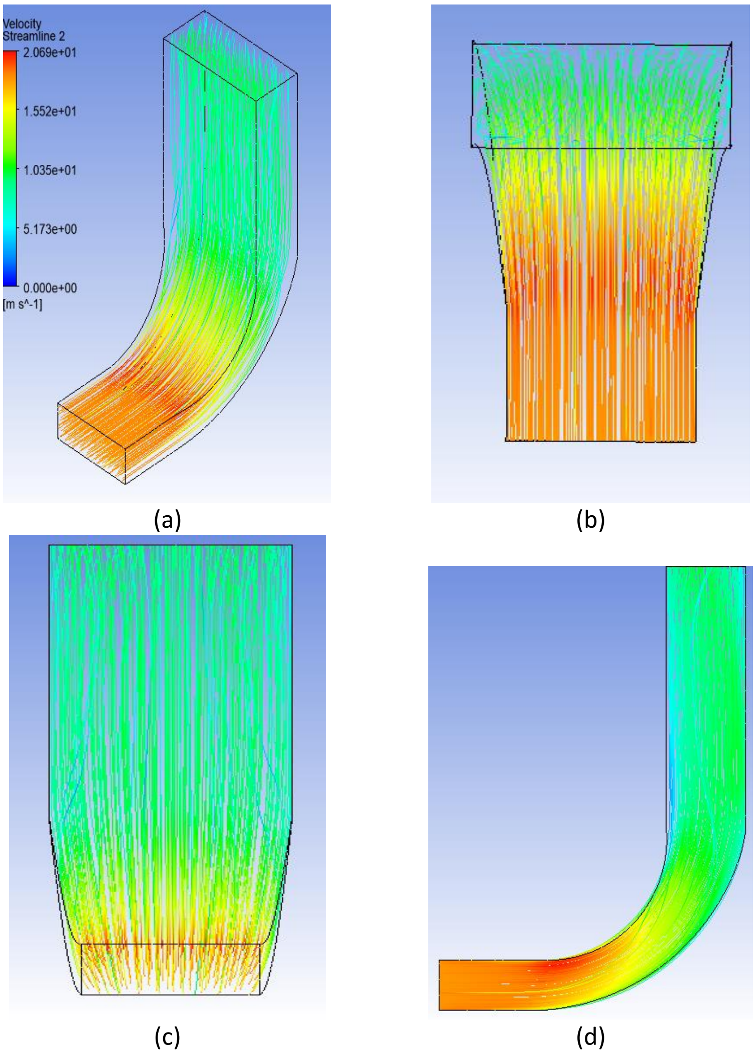

Fig. 9. 90° curve diffuser with the best pressure recovery (AR=2.16, 3D expansion x- and z- direction, Rein=8.163 x 10^4) (a) isometric (b) plan (c) frontal (d) side views

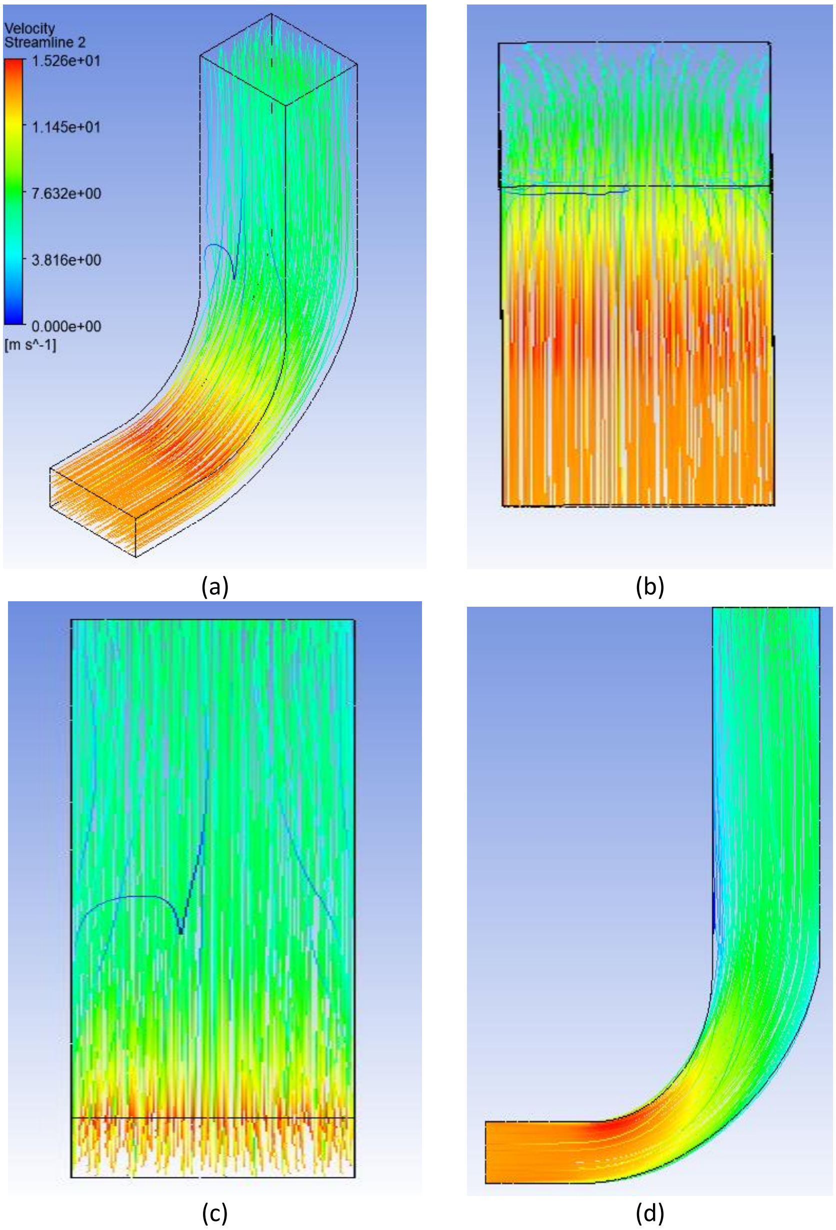

Fig. 10. 90° curve diffuser with the the best flow uniformity (AR=2.16, 2D expansion z- direction, Re_{in}=5.934 x 10^4) (a) isometric (b) plan (c) frontal (d) side views

Table 9
Performance status of 90° curve diffuser with AR= 1.2- 4.0 and Re_{in}= 5.934 x 10^4-1.738 x 10^5

Status of performances	Result	AR	Expansion direction	Re_{in}
Best pressure recovery (C_p)	0.384	2.16	3D expansion (x- and z- direction)	8.163 x 10^4
Worse pressure recovery (C_p)	0.011	4.00	2D expansion (x- direction)	8.163 x 10^4
Best flow uniformity (σ_{out})	2.33	2.16	2D expansion (z- direction)	5.934 x 10^4
Worse flow uniformity (σ_{out})	9.89	4.00	2D expansion (x- direction)	1.783 x 10^5

Table 10
Average performance expansion direction of 90° curve diffuser with AR= 1.2- 4.0 and Re_{in}= 5.934 x 10^4-1.738 x 10^5

Expansion direction	Pressure recovery coefficient, C_p	Flow uniformity index, σ_{out}
2D expansion (z- direction)	0.212	5.13
3-D expansion (x- and z- direction)	0.232	4.89
2D expansion (z-direction)	0.116	5.62

4. Conclusions

In conclusion, the effects of expansion direction, area ratio and inflow Reynolds Number on 90° curve diffuser performances have been successfully investigated with the optimum configuration been proposed. The main findings are highlighted as follows

i. Pressure recovery performance is governed more by AR, meanwhile flow uniformity is by Re_{in}. Optimum AR of 2.16 is proposed with low Re_{in} = 5.934 x 10^4 – 8.163 x 10^4 applied.
ii. Both 2D expansion (z- direction) and 3D expansion (x- and z- direction) provide comparable performances, thus the selection of a more appropriate model should be based upon the needs and restrictions of application.
iii. 2D inner wall expansion (x- direction) should as best eluded as it provides the most affected pressure recovery and flow uniformity performances of respectively up to 50% and 15%.
iv. 3D expansion (x- and z- direction), AR=2.16, Re_{in}=8.163 x 10^4 is the most optimum configuration to provide the highest pressure recovery of 0.384 (σ_{out}=3.33). Meanwhile, 2D expansion (z- direction), AR=2.16, Re_{in}=5.934 x 10^4 is the most optimum configuration to provide the most uniform flow of 2.33 (C_p=0.360).

Acknowledgement
This research was supported by Ministry of Higher Education through Fundamental Research Grant Scheme (FRGS/1/2018/TK03/UTHM/02/7). We also want to thank to the Universiti Tun Hussein Onn Malaysia (UTHM) for providing facilities to conduct the work.

References
[1] Gopaliya, Manoj Kumar, Mahesh Kumar, Shailendra Kumar, and Shiv Manjaree Gopaliya. "Analysis of performance characteristics of S-shaped diffuser with offset." *Aerospace Science and Technology* 11, no. 2-3 (2007): 130-135. https://doi.org/10.1016/j.ast.2006.11.003
[2] Cherry, Erica M., Angelina M. Padilla, Christopher J. Elkins, and John K. Eaton. "Three-dimensional velocity measurements in annular diffuser segments including the effects of upstream strut wakes." *International journal of heat and fluid flow* 31, no. 4 (2010): 569-575. https://doi.org/10.1016/j.ijheatfluidflow.2010.02.029
[3] Gan, Guohui, and Saffa B. Riffat. "Measurement and computational fluid dynamics prediction of diffuser pressure-loss coefficient." *Applied energy* 54, no. 2 (1996): 181-195. https://doi.org/10.1016/0306-2619(95)00078-X
[4] Gopaliya, Manoj Kumar, Piyush Goel, Sunil Prashar, and Anil Dutt. "CFD analysis of performance characteristics of S-shaped diffusers with combined horizontal and vertical offsets." *Computers & fluids* 40, no. 1 (2011): 280-290. https://doi.org/10.1016/j.compfluid.2010.09.027
[5] Husin, Azmi, Mohd Zulkifly Abdullah, Azmi Ismail, Ayub Ahmed Janvekar, Mohd Syakirin Rusdi, and Wan Mohd Amri Wan Mamat Ali. "Heat Transfer Performance of a Synthetic Jet Generated by Diffuser-Shaped Orifice." *Journal of Advanced Research in Fluid Mechanics and Thermal Sciences* 53, no. 1 (2019): 122-128.
[6] Hafez, Ahmed Hussein, Tamer Heshmat Mohamed Aly Kasem, Basman Elhadidi, and Mohamed Madbouly Abdelrahman. "Modelling Three Dimensional Unsteady Turbulent HVAC Induced Flow." *Journal of Advanced Research in Fluid Mechanics and Thermal Sciences* 87, no. 1 (2021): 76-90. https://doi.org/10.37934/arfmts.87.1.7690

[7] Nordin, Normayati. "Performance investigation of turning diffusers at various geometrical and operating parameters." PhD diss., Universiti Teknologi Petronas, 2016.
[8] Chong, T. P., P. F. Joseph, and P. O. A. L. Davies. "A parametric study of passive flow control for a short, high area ratio 90deg curved diffuser." *Journal of Fluids Engineering* 130, no. 11 (2008). https://doi.org/10.1115/1.2969447
[9] C.K. Nguyen, T.D. Ngo, P.A. Mendis, and J. C. K. Cheung. "A flow analysis for a turning rapid diffuser using CFD*." J. Wind Eng.* 108, (2006): 749-752.
[10] Ruzaini, M. S., N. Nordin, A. Sadikin, A. N. Mohammed, A. Sapit, K. Abdullah, Y. Ramli, and A. F. Idris. "Pressure recovery performance of 2-D turning diffuser by varying area ratios and inflow Reynolds numbers." In *IOP Conference Series: Materials Science and Engineering*, vol. 243, no. 1, p. 012029. IOP Publishing, 2017. https://doi.org/10.1088/1757-899X/243/1/012029
[11] Buhari, Rosnawati, Munzilah Md Rohani, and Mohd Ezree Abdullah. "Dynamic load coefficient of tyre forces from truck axles." In *Applied Mechanics and Materials*, vol. 405, pp. 1900-1911. Trans Tech Publications Ltd, 2013. https://doi.org/10.4028/www.scientific.net/AMM.405-408.1900
[12] Khong, Y. T., N. Nordin, S. M. Seri, A. N. Mohammed, A. Sapit, I. Taib, K. Abdullah, A. Sadikin, and M. A. Razali. "Effect of turning angle on performance of 2-D turning diffuser via Asymptotic Computational Fluid Dynamics." In *IOP Conference Series: Materials Science and Engineering*, vol. 243, no. 1, p. 012013. IOP Publishing, 2017. https://doi.org/10.1088/1757-899X/243/1/012013
[13] Fox, Robert W., and S. J. Kline. "Flow regimes in curved subsonic diffusers." *Journal of Fluids Engineering, Transactions of the ASME* 84, no. 3(1962): 303-312. https://doi.org/10.1115/1.3657307
[14] Shariff, Muhammad Zahid Firdaus, Normayati Nordin, Lim Chia Chun, Shamsuri Mohamed Rasidi, Raudhah Othman, and Sharifah Adzila. "Development of Performance Correlations using ACFD Method for 2-D Curved Diffuser." *CFD Letters* 12, no. 8 (2020): 1-16. https://doi.org/10.37934/cfdl.12.8.116
[15] Rasidi, Shamsuri, Suzairin Md Seri, Normayati Nordin, Muhammad Zahid Shariff, Nurul Fitriah Nasir, Sharifah Adzila, and Raudhah Othman. "Numerical Investigation of 180o Curved Diffuser Performance by Varying Geometrical and Operating Parameters." *CFD Letters* 12, no. 7 (2020): 100-109. https://doi.org/10.37934/cfdl.12.7.100109
[16] Huang, Lim Gim, Normayati Nordin, Lim Chia Chun, Nur Shafiqah Abdul Rahim, Shamsuri Mohamed Rasidi, and Muhammad Zahid Firdaus Shariff. "Effect of Turbulence Intensity on Turning Diffuser Performance at Various Angle of Turns." *CFD Letters* 12, no. 1 (2020): 48-61.
[17] Tham, Wei Xian, Normayati Nordin, Azian Hariri, Nurul Fitriah Nasir, Norasikin Mat Isa, Musli Nizam Yahya, and Suzairin Md Seri. "Asymptotic computational fluid dynamic (ACFD) study of three-dimensional turning diffuser performance by varying angle of turn." *International Journal of Integrated Engineering* 11, no. 5 (2019): 109-118.
[18] Zhang, Wei-Li, Doyle D. Knight, and Don Smith. "Automated design of a three-dimensional subsonic diffuser." *Journal of Propulsion and Power* 16, no. 6 (2000): 1132-1140. https://doi.org/10.2514/2.5688
[19] Sedlár, Milan, and Jaromır Prıhoda. "Investigation of flow phenomena in curved channels of rectangular crosssection." *Engineering Mechanics* 14, no. 6 (2007): 387-397.
[20] Nordin, Normayati, Vijay R. Raghavan, Safiah Othman, and Zainal Ambri Abdul Karim. "Compatibility of 3-D turning diffusers by means of varying area ratios and outlet-inlet configurations." *ARPN Journal of Engineering and Applied Sciences* 7, no. 6 (2012): 708-713.
[21] Gan, Guohui, and Saffa B. Riffat. "Measurement and computational fluid dynamics prediction of diffuser pressure-loss coefficient." *Applied energy* 54, no. 2 (1996): 181-195. https://doi.org/10.1016/0306-2619(95)00078-X
[22] Wang, Yi-Chun, Jui-Cheng Hsu, Ping-Chi Kuo, and Yung-Chun Lee. "Loss characteristics and flow rectification property of diffuser valves for micropump applications." *International Journal of Heat and Mass Transfer* 52, no. 1-2 (2009): 328-336. https://doi.org/10.1016/j.ijheatmasstransfer.2008.06.010
[23] Mohamed, Mohamed S., Berge Djebedjian, and M. M. Rayan. "Experimental and Numerical Studies of Flow in a Logarithmic Spiral Curved Diffuser." In *Proceedings, FEDSM '2000, ASME Fluids Engineering Summer Meeting Conference*, pp. 1-8. 2000.
[24] Gopaliya, Manoj Kumar, and K. K. Chaudhary. "CFD analysis of performance characteristics of Y-shaped diffuser with combined horizontal and vertical offsets." *Aerospace Science and Technology* 14, no. 5 (2010): 338-347. https://doi.org/10.1016/j.ast.2010.02.008
[25] Gopaliya, Manoj Kumar, Piyush Goel, Sunil Prashar, and Anil Dutt. "CFD analysis of performance characteristics of S-shaped diffusers with combined horizontal and vertical offsets." *Computers & fluids* 40, no. 1 (2011): 280-290. https://doi.org/10.1016/j.compfluid.2010.09.027
[26] El-Askary, W. A., and M. Nasr. "Performance of a bend–diffuser system: Experimental and numerical studies." *Computers & fluids* 38, no. 1 (2009): 160-170. https://doi.org/10.1016/j.compfluid.2008.01.003